Inclusion of copper oxide nanoparticles and β-CD polymer for the enhancement of electrocatalytic property of reduced graphene oxide nanosheets and its sensing applications
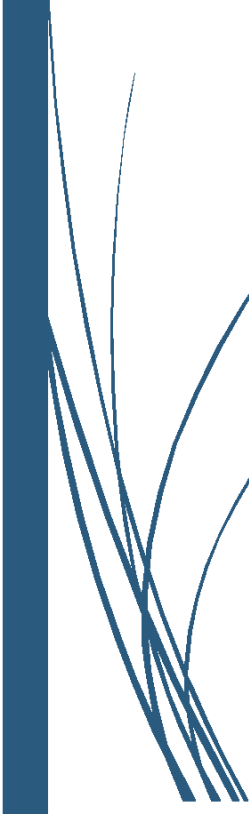
CHAPTER VII

INCLUSION OF COPPER OXIDE NANOPARTICLES AND β-CD POLYMER FOR THE ENHANCEMENT OF ELECTROCATALYTIC PROPERTY OF REDUCED GRAPHENE OXIDE NANOSHEETS AND ITS SENSING APPLICATIONS

This chapter includes:

- ❖ Introduction

- ❖ Materials and methods

- ❖ Functional and Structural characterization of various concentrations of rGONS/β-CD/CuO nanocomposite

- ❖ Morphological analysis

- ❖ Elemental analysis

- ❖ Electrocatalytic analysis for the sensing of nitrophenol isomers

- ❖ Conclusion

- ❖ References

7.1. INTRODUCTION

In recent years, graphene-based nanocomposites have received much attention in various fields including electrocatalysis [1]. Graphene has been generally recognized as a basic building block of all the graphitic materials and it has a high mechanical strength, large surface area and good electrochemical activity than the other carbon based nanomaterials such as carbon nanotubes [2]. The stability of graphene is found to be feeble in aqueous medium due to the strong π-π restacking nature of layers of graphene sheets into graphite [3]. Hence, the stability of graphene sheets can be enhanced by incorporating the various micro or nanomaterials including conducting polymer [4-5], metal/metal alloy/metal oxide nanoparticles [6-9] and supramolecular

adducts [10]. The graphene based nanocomposites have been widely employed as an electrode material for determination of highly toxic environmental pollutants [11-15].

Different types of polymer and wide variety of nanomaterials have been employed with graphene sheets to enhance the dispersion ability and catalytic activity of graphene sheets. In this chapter, β-cyclodextrin (β-CD) polymer is used as an appropriate dispersing agent and has effectively enhanced the dispersion ability of graphene sheets in aqueous medium, thereby avoiding the re-stacking of individual graphene sheets [16]. The exciting hydrophilic exterior and hydrophobic interior cavity characteristics of β-CD allow the cyclodextrin molecules to form the stable nanocomposite with graphene sheets. Furthermore, the intercalation of exclusive properties of β-CD can improve the electrocatalytic activity of the graphene sheets.

The electrocatalytic properties of graphene sheets can be further enhanced by the inclusion of copper oxide nanoparticles. These copper oxide (CuO) nanoparticles have gained much attention in the electrochemical society due to its high surface to volume ratio and excellent electrocatalytic activity and non-toxicity [17,18]. Because of these significant properties, copper oxide nanoparticles have been widely employed in various fields such as photocatalysis [19], sensors [20] and energy storage devices [21]. Henceforth, the inclusion of copper oxide nanoparticles with β-cyclodextrin functionalized graphene sheets would further enhance the electrocatalytic behaviour of graphene sheets.

Copper oxide nanoparticles decorated β-cyclodextrin functionalized reduced graphene oxide nanosheets via wet chemical methodology is synthesized and employed for the electrochemical detection of nitrophenol isomers. These isomers are kind of nitro compounds, which are categorized as hazardous environmental pollutant and are widely existed in pharmaceuticals, dyes and pesticides. Nitrophenol can survive in the environment for a long period of time due to its excellent stability and may cause unwanted health defects [22]. Hence, it is significantly important to produce a facile, cost-efficient and reliable material for the detection of nitrophenol isomers.

7.2. MATERIALS AND METHODS

The β-cyclodextrin functionalized copper oxide (CuO) nanoparticles decorated reduced graphene oxide nanosheets (rGONS/β-CD/CuO) are synthesized by wet chemical method. Chemically functionalized reduced graphene oxide nanosheets/ β-cyclodextrin nanosheets are synthesized by taking 50 mg of graphene oxide and 0.6 g of β-cyclodextrin powder and dispersed in an aqueous solution. The dispersed β-cyclodextrin polymer solution is added into graphene oxide suspension followed by the addition of 20 μL of hydrazine hydrate and 300 μL of ammonia as a reducing agent and stirred for 4 hours at 80˚C. The centrifuged rGONS/β-CD reaction suspension is then dispersed in a 50 ml of water for the decoration of copper oxide nanoparticles [10] [23]. 0.002 M of Copper II acetate monohydrate ($CH_3COO_2C_4.H_2O$) is taken and dispersed in a 50 mL of water. The dispersed copper II acetate monohydrate ($CH_3COO_2C_4.H_2O$) solution is then added into the rGONS/β-CD suspension followed by the addition of sodium borohydrate ($NaBH_4$) as a reducing agent and stirred for 4 hours at 80˚C. The synthesized rGONS/β-CD/CuO nanocomposite is washed thoroughly using deionised water and dried under vacuum for 4 hours [24-25].

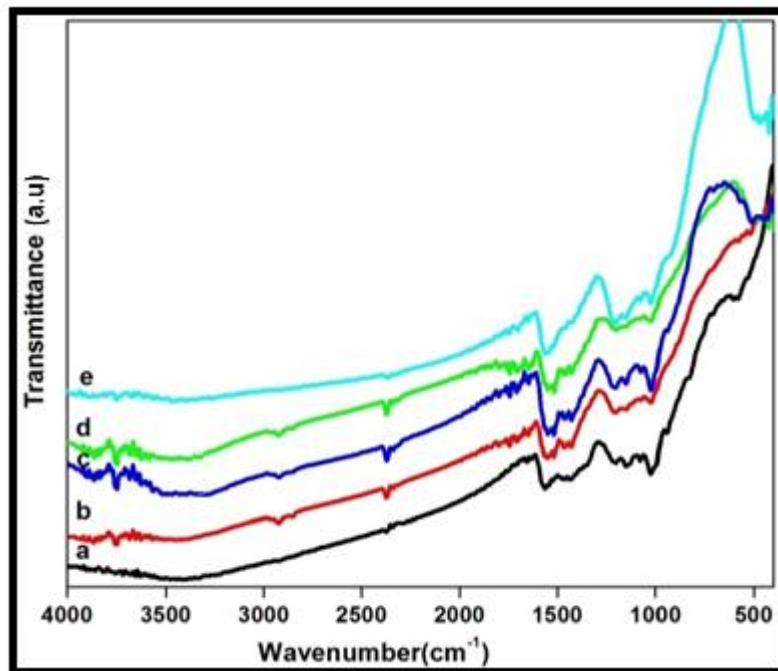## 7.3. RESULTS AND DISCUSSION

7.3.1. FT-IR SPECTRAL ANALYSIS

Figure.7.1. FT-IR spectra of copper oxide nanoparticles decorated β-cyclodextrin functionalized reduced graphene oxide nanosheets using (a) 0.002 M (b) 0.004 M (c) 0.006 M (d) 0.008 M and (e) 0.01 M concentrations of copper II acetate monohydrate

Figure.7.1.(a-e) shows the Fourier transform infrared (FT-IR) spectra of copper oxide nanoparticles decorated β-cyclodextrin functionalized reduced graphene oxide nanosheets (rGONS/β-CD/CuO) using different concentrations (0.002 M, 0.004 M, 0.006 M, 0.008 M and 0.01 M) of copper II acetate monohydrate. In the Figure.7.1.(a-e), the absorption bands observed at 3766.77 cm^{-1}, 3465.97 cm^{-1} may be corresponding to the O-H stretching and bending vibrations of water molecules in the reduced graphene oxide nanosheets and β-cyclodextrin polymer [23] [26]. The absorption bands obtained at 2924.62 cm^{-1} and 2373.41 cm^{-1} may be attributed to the bending vibrations of C-H functional groups in the β-cyclodextrin polymer. The bands observed at 1427.78 cm^{-1}, 1023.45 cm^{-1} and 1213.56 cm^{-1} corresponds to the C-O (carboxy), O-H and C-O (epoxy) vibrations of β-cyclodextrin polymer on the reduced graphene oxide nanosheets [23] [26-27]. The band observed at 1582.01 cm^{-1} may arises due to the

presence of enhanced benzene ring vibrations of restacking nature of C=C cfunctional group in reduced graphene oxide nanosheets [28]. The band observed between 500 cm^{-1} to 1000 cm^{-1} confirms the presence of copper oxide nanoparticles on the surface rGO/β-CD nanosheets [29].

The absence of absorption band corresponding to the carboxylic functional group of graphene oxide nanosheets at 1725 cm^{-1} confirms the reduction of graphene oxide nanosheets during the synthesis of rGONS/β-CD/CuO nanocomposites and the inclusion of cu^{2+} ions [30]. The appearance of benzene ring absorption band in the FT-IR spectra of rGONS/β-CD/CuO nanocomposites in comparison with that of the FT-IR spectra of GO and rGO nanosheets with reference to the Figure.3.1. in the chapter 3, confirms the functionalization of β-cyclodextrin polymer with the reduced graphene oxide nanosheets and the restoration of combined structure of reduced graphene oxide nanosheets [28]. It is observed from the Figure.7.1.(a-e) that the red shift occurs in the O-H functional groups of water molecules, thereby confirming the intermolecular interactions between rGO nanosheets and β-CD polymer (i.e) hydrogen bonding thereby change the water adsorption behaviour of reduced graphene oxide nanosheets due to the excellent hydrophilic nature of β-CD polymer [23] [26-27]. The change in the intensities of all the vibrational bands of β-cyclodextrin polymer and reduced graphene oxide nanosheets with the increase in the concentration of copper II acetate monohydrate from 0.002 M to 0.01 M confirms that the copper oxide nanoparticles are uniformly and physically grafted on the surface of rGONS/β-CD nanosheets [31].
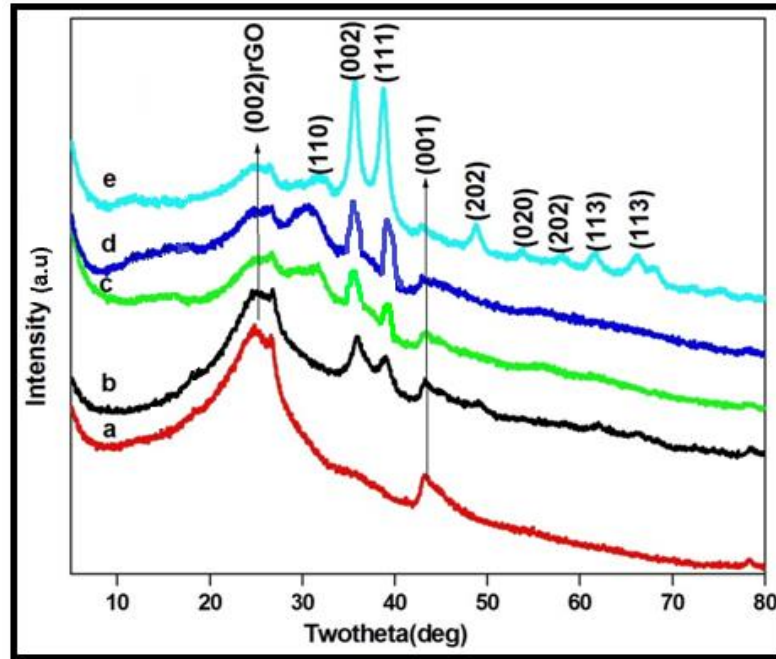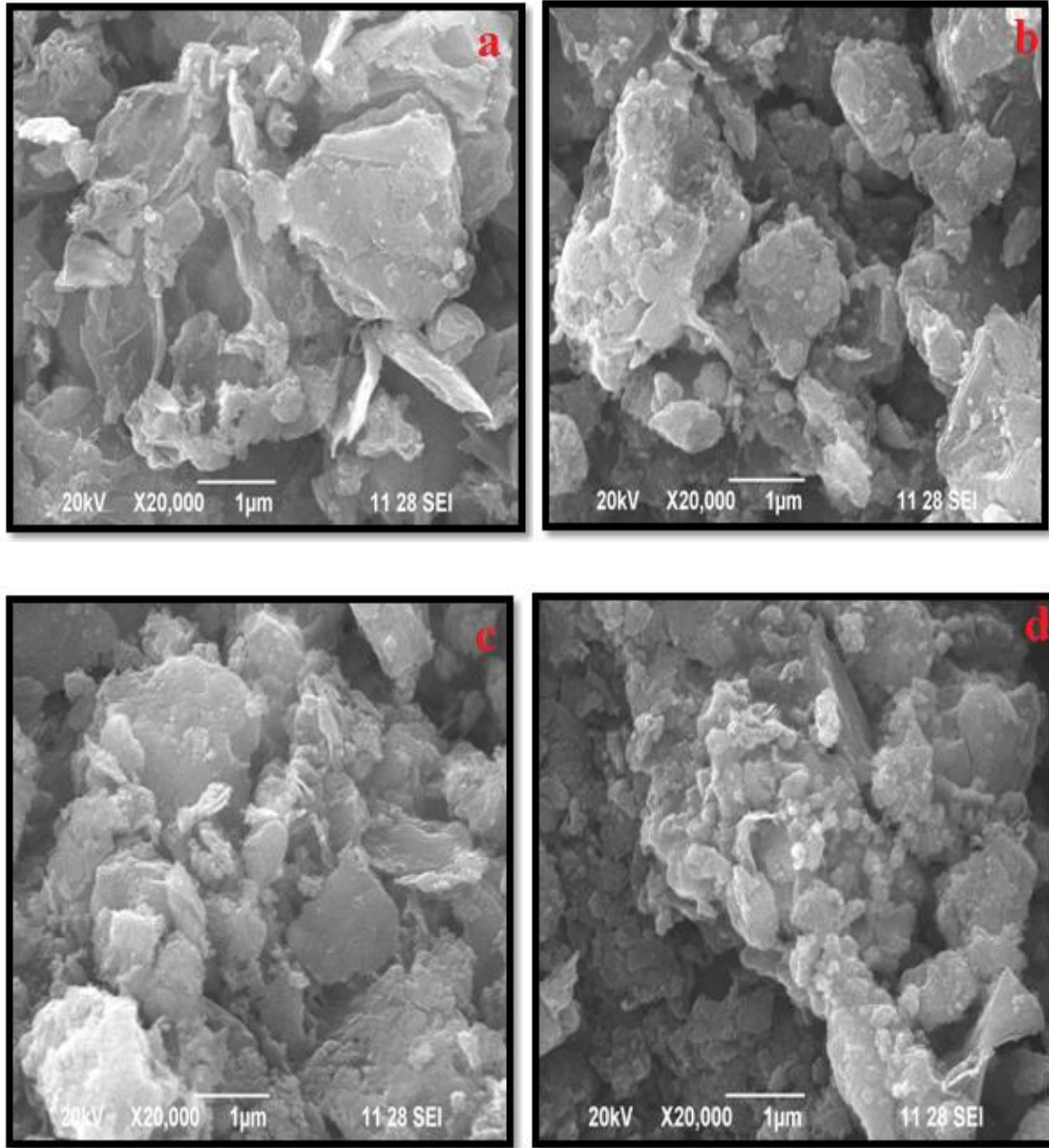
7.3.2. STRUCTURAL ANALYSIS

Figure.7.2. XRD spectra of copper oxide nanoparticles decorated β-cyclodextrin functionalized reduced graphene oxide nanosheets using (a) 0.002 M (b) 0.004 M (c) 0.006 M (d) 0.008 M and (e) 0.01 M concentrations of copper II acetate monohydrate

Figure.7.2.(a-e) shows the X-ray diffraction (XRD) pattern of copper oxide nanoparticles decorated β-cyclodextrin functionalized reduced graphene oxide nanosheets (rGONS/β-CD/CuO) using different concentrations (0.002 M, 0.004 M, 0.006 M, 0.008 M and 0.01 M) of copper II acetate monohydrate. The X-ray diffraction pattern shows the prominent diffraction peaks at 31.5˚, 35.6˚, 38.7˚, 48.7˚, 53.6˚, 57.9˚, 61.4˚ and 66.1˚ and are assigned to the (110), (111), (200), (202), (020), (021), (113) and (311) diffraction planes of monoclinic phase of copper oxide nanoparticles and are indexed with the standard JCPDS card number (48-1548) [32]. The X-ray diffraction pattern of rGONS/β-CD/CuO nanocomposites shows the broad diffraction peak at 24.7˚, which corresponds to the (002) diffraction plane of reduced graphene oxide nanosheets. The broadness in the diffraction peak may be ascribed to the increase in the inter-layer spacing value of rGO nanosheets by the inclusion of β-CD polymer which thereby inhibits the restacking of rGO layers [28]. The crystallite size of the copper oxide nanoparticles decorated on the surface of rGO/β-CD nanosheets for the different

concentrations (0.002 M, 0.004 M, 0.006 M, 0.008 M and 0.01 M) of copper II acetate monohydrate are calculated using the Debye-Scherrer's equation [33] and are found to be 8.6 nm, 16.9 nm, 21.6 nm, 22.5 nm and 24.3 nm respectively.

It is observed from the XRD analysis that the intensity of crystalline peaks corresponding to copper oxide nanoparticles are increasing with the increase in the copper II acetate monohydrate concentrations from 0.002 M to 0.01 M, thereby confirming the decoration of high crystalline copper oxide nanoparticles on the surface of β-cyclodextrin functionalized reduced graphene oxide nanosheets [31]. It is also observed from the XRD analysis that the diffraction peak corresponding to the β-cyclodextrin functionalized reduced graphene oxide nanosheets as discussed in chapter 3 are only observed for the lower concentration of (0.002 M and 0.004 M) rGONS/β-CD/CuO nanocomposites, thereby confirming the successful reduction of GO nanosheets into rGO nanosheets. The strong chemical functionalization of β-CD polymer with the rGO nanosheets and the decoration of small amount of copper oxide nanoparticles on the surface of rGO/β-CD nanosheets in the synthesized rGONS/β-CD/CuO nanocomposites are also evidenced in Figure.7.2 (a & b). With the further increase in the concentration of copper II acetate monohydrate from 0.006 M to 0.01 M, the diffraction peak intensity of rGO/β-CD nanosheet decreases and may be due to the decoration of copper oxide nanoparticles on the surface of rGO/β-CD nanosheets [31]. This causes the copper oxide nanoparticles to be intercalated with the adjacent sheets of rGONS/β-CD, thereby increasing the inter-layer spacing and broadening of the X-ray diffraction peak.

7.3.3. SEM ANALYSIS

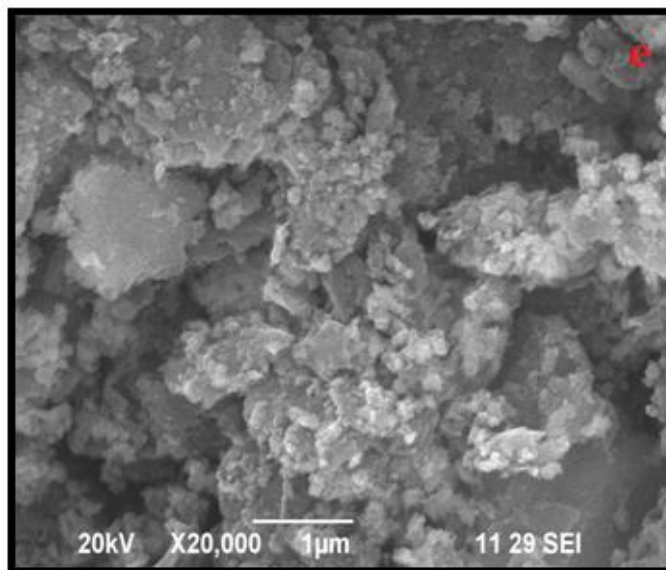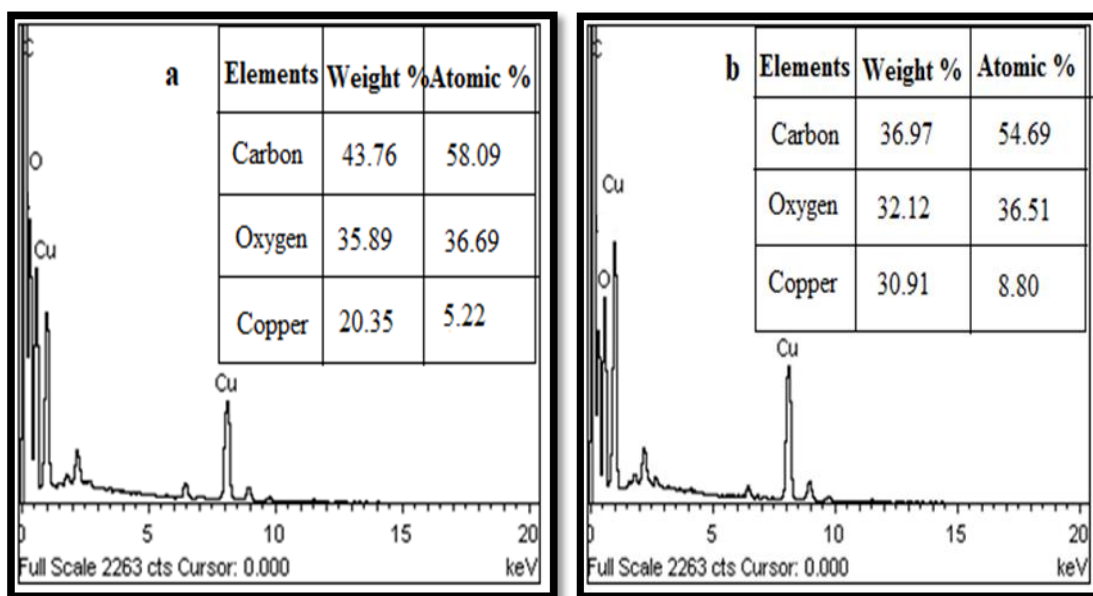**Figure.7.3. SEM images of copper oxide nanoparticles decorated β-cyclodextrin functionalized reduced graphene oxide nanosheets using (a) 0.002 M (b) 0.004 M (c) 0.006 M (d) 0.008 M and (e) 0.01 M concentrations of copper II acetate monohydrate**

Figure.7.3.(a-e) shows the scanning electron micrographs (SEM) of copper oxide nanoparticles decorated β-cyclodextrin functionalized reduced graphene oxide nanosheets synthesized using five different concentrations (0.002 M, 0.004 M, 0.006 M, 0.008 M and 0.01 M) of copper II acetate monohydrate. The micrographs of rGONS/β-CD/CuO nanocomposite show the spherical shaped copper oxide nanoparticles are well dispersed on the surface and edges of the rGO/β-CD nanosheets, that indicates a strong interaction between rGO/β-CD nanosheets and copper oxide nanoparticles which could also be evidenced from HRTEM analysis [29] [34-35]. The micrographs of rGONS/β-CD/CuO nanocomposites also shows that the dispersion of copper oxide nanoparticles on the surface of rGO/β-CD nanosheets are found to be increased with the increase in the concentrations of copper II acetate monohydrate from 0.002 M to 0.004 M without agglomeration [36]. With the further increase in the concentration of copper II acetate monohydrate above 0.004 M, the dispersion of copper oxide nanoparticles on the surface of rGO/β-CD nanosheet is found to be aggregated, which indicates that the high loading concentration of copper oxide nanoparticles on the rGONS/β-CD surface leads to aggregation and thereby confirming the saturation of accommodating ability of functional groups of rGONS/β-CD [31] [37]. Hence it reduces the contact surface area

with the nitrophenol isomers due to the agglomerated copper oxide nanoparticles on the rGONS/β-CD surface and thereby decreasing the electrochemical sensing property of rGONS/β-CD/CuO nanocomposites.

The SEM images of rGONS/β-CD/CuO nanocomposites show the wrinkled morphology of β-cyclodextrin functionalized reduced graphene oxide nanosheets, thereby confirming the formation of β-CD functionalized rGONS as evidenced from the SEM images of rGONS/β-CD as discussed in the chapter 3 [34]. The wrinkled surface morphology of rGONS/β-CD provides a high specific surface area to enhance the number of copper oxide nanoparticles decoration and the excellent host guest property to enhance the number of nitrophenol isomers attachments with the surface of rGONS/β-CD/CuO nanocomposites during the electrochemical sensing analysis, thereby enhances the catalytic and sensitivity of synthesized rGONS/β-CD/CuO nanocomposites [10] [38]. Among the various concentrations of copper II acetate monohydrate, the rGONS/β-CD/CuO nanocomposites synthesized using 0.004 M concentration of copper II acetate monohydrate only shows the large number of uniformly deposited copper oxide nanoparticles and hence it is chosen as the good electrode material for the electrochemical sensing of nitrophenol isomers.
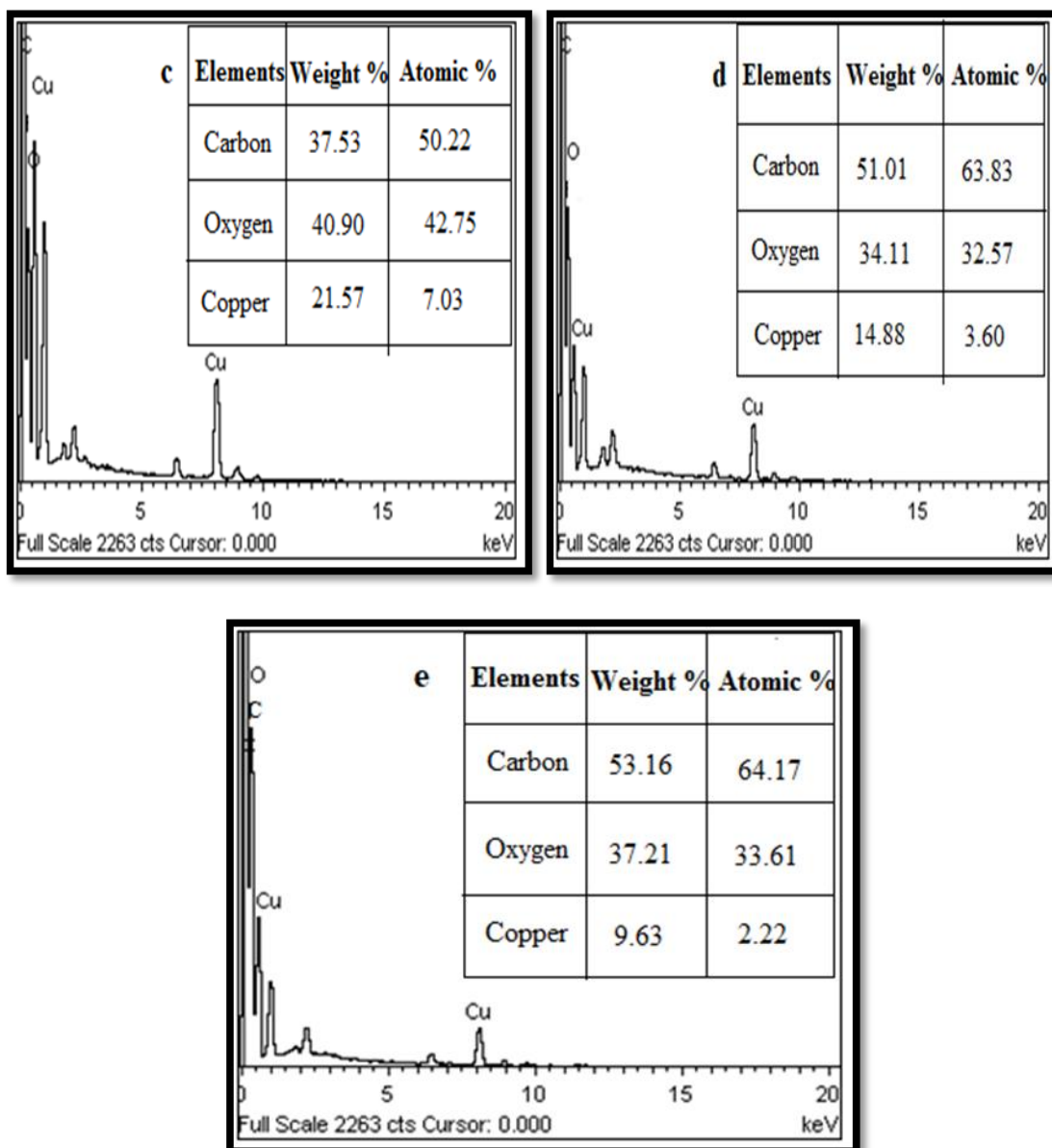
7.3.4. EDAX ANALYSIS

a	Elements	Weight %	Atomic %
	Carbon	43.76	58.09
	Oxygen	35.89	36.69
	Copper	20.35	5.22

Full Scale 2263 cts Cursor: 0.000   keV

b	Elements	Weight %	Atomic %
	Carbon	36.97	54.69
	Oxygen	32.12	36.51
	Copper	30.91	8.80

Full Scale 2263 cts Cursor: 0.000   keV

c	Elements	Weight %	Atomic %
	Carbon	37.53	50.22
	Oxygen	40.90	42.75
	Copper	21.57	7.03

d	Elements	Weight %	Atomic %
	Carbon	51.01	63.83
	Oxygen	34.11	32.57
	Copper	14.88	3.60

e	Elements	Weight %	Atomic %
	Carbon	53.16	64.17
	Oxygen	37.21	33.61
	Copper	9.63	2.22

Figure.7.4. EDAX spectra of copper oxide nanoparticles decorated β-cyclodextrin functionalized reduced graphene oxide nanosheets using (a) 0.002 M (b) 0.004 M (c) 0.006 M (d) 0.008 M and (e) 0.01 M concentrations of copper II acetate monohydrate

The EDAX analysis is used to investigate the atomic percentage and composite formation in the synthesized composition. The EDAX spectra of copper oxide nanoparticles decorated β-cyclodextrin functionalized reduced graphene oxide nanosheets using five various concentrations (0.002 M, 0.004 M, 0.006 M, 0.008 M and 0.01 M) of copper II acetate monohydrate are shown in the Figure.7.4.(a-e). The atomic and weight percentage of elements such as oxygen, carbon and copper are shown in the

inset of the Figure.7.4.(a-e). The presence of carbon, oxygen and copper elements confirms the synthesis of rGONS/β-CD/CuO nanocomposite without any impurities [25].
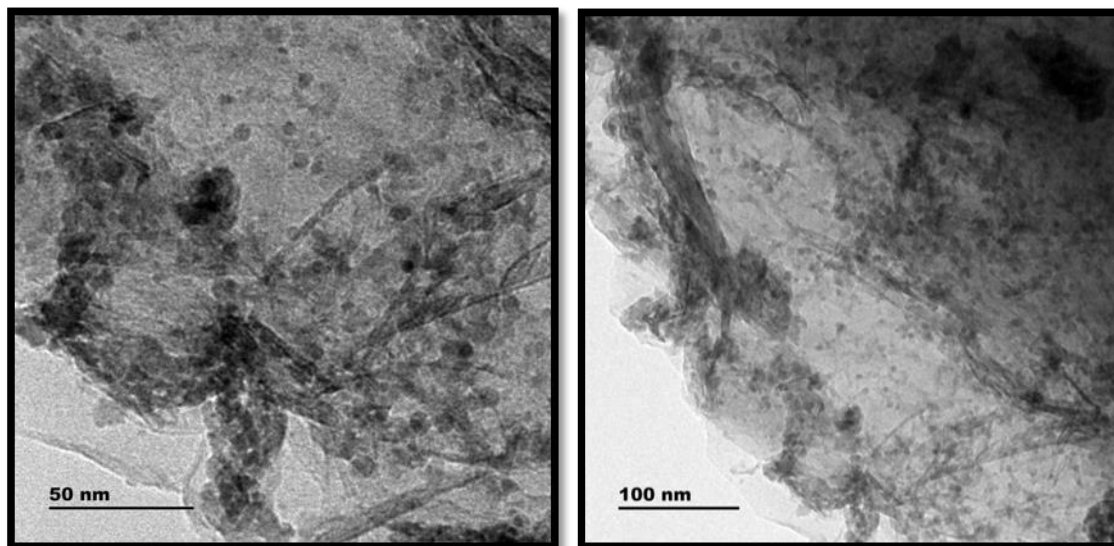
7.3.5. HRTEM ANALYSIS

Figure.7.5. HRTEM images of copper oxide nanoparticles decorated β-cyclodextrin functionalized reduced graphene oxide nanosheets synthesized using 0.004 M concentration of copper II acetate monohydrate

The high resolution transmission electron micrographs (HRTEM) of the synthesized rGONS/β-CD/CuO nanocomposite using 0.004 M concentration of copper II acetate monohydrate are shown in the Figure.7.5. The HRTEM images depicts that the synthesized rGO/β-CD nanosheets are wrinkled, crumpled and less transparent [23] [26], which may be due to the impact of chemical functionalization of hydrophillic β-cyclodextrin polymer across the basal plane of rGO nanosheets and thereby prevents the aggregations and restacking of reduced graphene oxide nanosheets [23] [26]. This demostrates that the synthesized rGO nanosheets are quite thin and well exfoliated [31]. It is observed from the Figure.7.5 that the appearance of black spots on the surface of rGO/β-CD nanosheets confirms the formation of well distributed copper oxide nanoparticles, which is also evidenced in the SEM analysis [35-36]. The distributions of copper oxide nanoparticles are homogeneous and non-agglomerated, which may be due to the impact of hydrophilic property of functionalized β-cyclodextrin polymer on the

enhancement of dispersion ability of synthesized rGO/β-CD nanosheets and the strong interaction between the copper oxide nanoparticles and rGO/β-CD nanosheets [35].
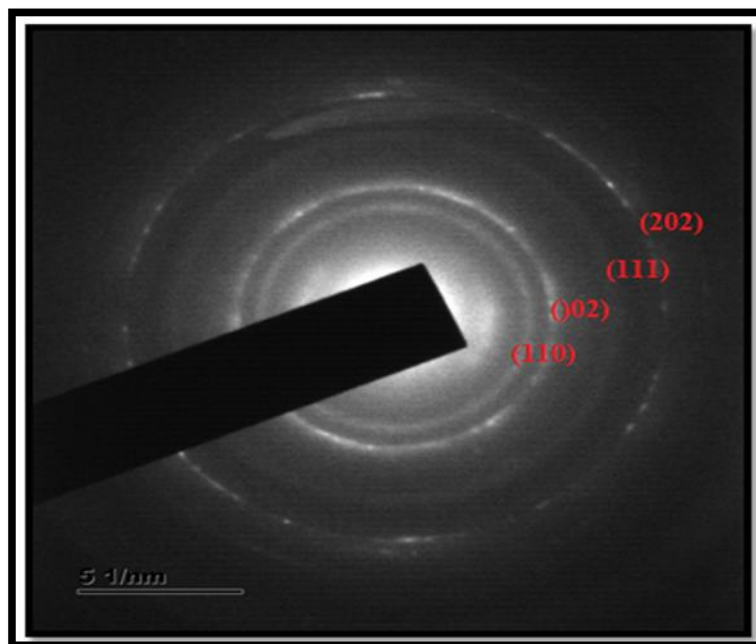
7.3.6. SAED ANALYSIS

Figure.7.6. SAED pattern of copper oxide nanoparticles decorated β-cyclodextrin functionalized reduced graphene oxide nanosheets synthesized using 0.004 M concentration of copper II acetate monohydrate

The selected area electron diffraction pattern (SAED) of the synthesized rGONs/β-CD/CuO nanocomposites using 0.004 M concentration of copper II acetate monohydrate is shown in Figure.7.6. It is observed from the Figure.7.6 that there are four discrete bright rings, which correspond to the successful decoration of well crystalline copper oxide nanoparticles on the surface of rGO/β-CD nanosheets. Each rings corresponds to the (110), (111), (200) and (202) diffraction planes of monoclinic phase of copper oxide nanoparticles, which could also be evidenced from XRD analysis.

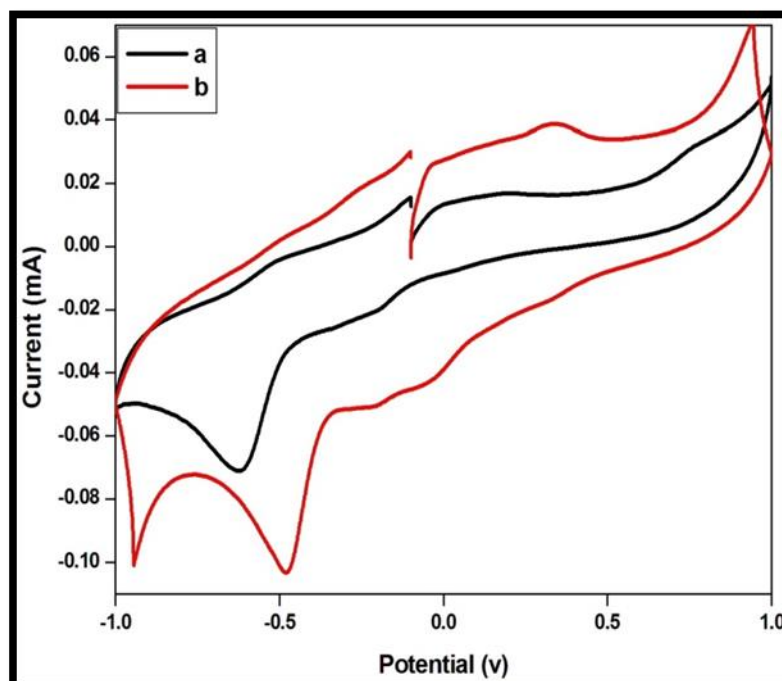## 7.4. ELECTROCHEMICAL BEHAVIOUR OF MODIFIED ELCTRODES

Figure.7.7. Cyclic voltagramm of 230 μM of o-NP at (a) rGONS/CuO/GCE (b) rGONS/β-CD/CuO/GCE in PBS solution at the scan rate of 10 mV/s

To study the electrochemical behaviour of rGONS/CuO and rGONS/β-CD/CuO nanocomposite modified glassy carbon electrodes (GCE) towards the electrocatalytic reduction and oxidation of ortho-nitrophenol (o-NP), the concentration of o-NP is varied form 100 μM to 240 μM. The maximum redox current response is obtained for the 230 μM of o-NP and the results are presented in the Figure.7.7.(a and b). It shows the cyclic voltammetric response of the rGONS/CuO and rGONS/β-CD/CuO nanocomposite modified glassy carbon electrodes (GCE) towards the electrocatalytic reduction and oxidation of 230 μM of ortho-nitrophenol (o-NP) at the scan rate of 10 mV/s in the 0.1 M of phosphate buffer solution (pH 5), respectively. The cyclic voltagramm of rGONS/CuO/GCE and rGONS/β-CD/CuO/GCE shows a prominent redox peak at the potential of -0.62 V, +0.20 V and -0.48, + 0.33 V with the corresponding redox peak current of -0.071 mA, +0.017 mA and -0.102 mA, +0.038 mA, respectively, which indicates the excellent electrochemical activity of both the modified electrode towards the detection of o-NP. It is observed from the Figure.7.7.(a & b) that the redox peak current corresponds to the reduction and oxidation of o-NP using rGONS/β-CD/CuO/GCE is higher than the rGONS/CuO/GCE,

thereby confirming the impact of β-cyclodextrin polymer functionalized with rGONS on the electrocatalytic reduction and oxidation of o-NP [39] .

The detection peak current of o-NP for rGONS/β-CD/CuO/GCE is higher than the rGONS/β-CD/GCE (as discussed in chapter 3), due to the impact of copper oxide nanoparticles on the electrocatalytic reduction and oxidation of o-NP. It is revealed from the electrocatalytic analysis that the enhancement in the redox peak current may be attributed to high electrical conductivity of rGONS, supra molecular recognition ability of β-cyclodextrin polymer, high catalytic ability of copper oxide nanoparticles, high specific surface area and excellent electrocatalytic property of rGONS/β-CD and the synergistic effect between β-CD functionalized rGO nanosheets and copper oxide nanoparticles [10] [29] [39]. The high specific surface area of rGONS/β-CD/CuO/GCE enhances the number of absorption of copper oxide nanoparticles, which may be due to the rough surface morphology of rGONS/β-CD nanosheets by the functionalized cyclodextrin polymer as evidenced from SEM analysis. The cyclodextrin polymer not only enhances the surface area but also provides the host guest inclusion complexes property to enhance the number of nitrophenol sites attachment with the rGONS/ β-CD/CuO nanocomposites surface [39].

It is confirmed from the electrochemical characterization studies that the copper oxide nanoparticles decorated on the β-cyclodextrin functionalized reduced graphene oxide nanosheets shows the good electrochemical sensing behaviour than the other modified electrodes (bare/GCE, GO/GCE, rGONS/β-CD/GCE and rGONS/CuO/GCE). Further the enhancement in the electrochemical property of rGONS/β-CD/CuO nanocomposites is achieved by optimizing the electrochemical parameters such as concentration of CuO on the rGONS/β-CD, pH and scan rate, etc.

7.5. ELECTROCHEMICAL DETECTION OF NITROPHENOL ISOMERS

The synthesized rGONS/β-CD/CuO nanocomposites is employed for the sensitive electrochemical detection of nitrophenol isomers such as ortho-, para-, and meta-nitrophenol. The maximum electrocatalytic activity towards the detection of ortho-, para-, meta-nitrophenol can be achieved by investigating the electrochemical parameters such as pH of the electrolyte medium, concentration of the rGONS/ β-CD/CuO nanocomposite and the scan rate of electrochemical reaction.

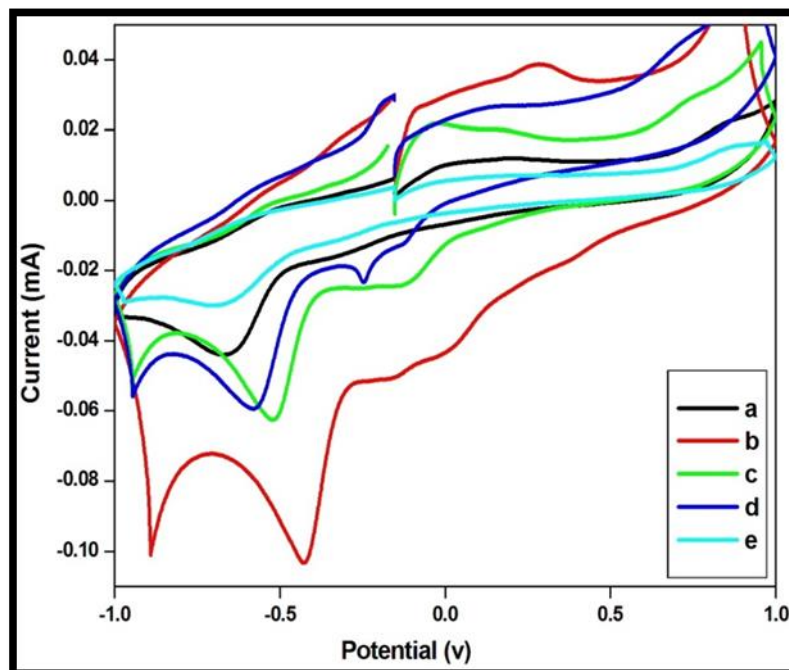### 7.5.1. Effect of rGONS/β-CD/CuO concentration on electrocatalytic activity

Figure.7.8. Cyclic voltagramm of 230 μM of o-NP at (a) 0.002 M (b) 0.004 M (c) 0.006 M (d) 0.008 M (e) 0.01 M concentration of copper oxide nanoparticles decorated β-cyclodextrin functionalized reduced graphene oxide nanosheets in PBS solution

Figure.7.8.(a-e) shows the electrocatalytic activity of o-nitrophenol for the synthesized (a) 0.002 M, (b) 0.004 M, (c) 0.006 M, (d) 0.008 M and (e) 0.01 M concentration of rGONS/β-CD/CuO nanocomposite modified GCE in 0.1 M of phosphate buffer solution (PBS) containing 230 μM of o-nitrophenol at the scan rate of 10 mV/s. It is observed from the Figure.7.8.(a-e) that all the concentrations (0.002 M, 0.004 M, 0.006 M, 0.008 M and 0.01 M) of copper oxide nanoparticles decorated β-cyclodextrin functionalized reduced graphene oxide nanosheets modified GCE shows the good electrochemical response towards the detection of o-nitrophenol. The cyclic voltagramm of 0.002 M concentration of rGO/β-CD/CuO nanocomposites modified GCE shows the lower reduction peak current, which may be due to the deficient electro-catalysis of rGONS/β-CD/CuO with the o-nitrophenol isomer [40] [31]. But with the further increment in the concentration of copper II acetate monohydrate from 0.002 M to 0.004 M, the rGONS/β-CD/CuO/GCE exhibits a higher electrocatalytic

reduction peak current, thereby confirming the higher catalytic activity of synthesized nanocomposites with the o-nitrophenol. The increase in the redox peak current may be attributed to the increase in the concentration of copper oxide nanoparticles decorated on the rGONS/β-CD surface [40] [31] and also the excellent synergistic behaviour of copper oxide nanoparticles towards o-nitrophenol. Furthermore, with the continuous increase in the concentrations of copper II acetate monohydrate from 0.006 M to 0.01 M, the peak current corresponding to reduction of o-nitrophenol is found to be decreased, which might be due to the aggregation of copper oxide nanoparticles decorated on the rGONS/β-CD surface and also decreases the electrocatalytic activity between electrode surface and o-NP site, which is as also evidenced from SEM and EDAX analysis [40] [31]. It is confirmed from the electrocatalytic analysis that the rGONS/β-CD/CuO nanocomposite synthesized with 0.004 M concentration of copper II acetate monohydrate has better electrochemical behaviour and higher reduction peak current than the other concentrations of copper oxide modified rGONS/β-CD surface. Hence it is chosen as an electrode modifying material for the quantitative detection of ortho-, para- and meta-nitrophenol isomers.
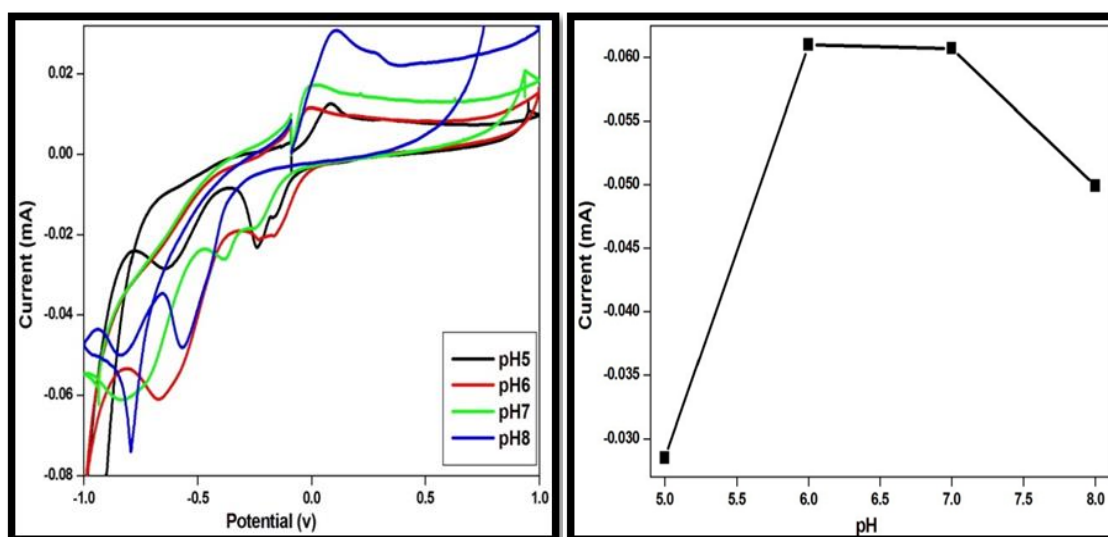
### 7.5.2 Effect of electrolyte pH
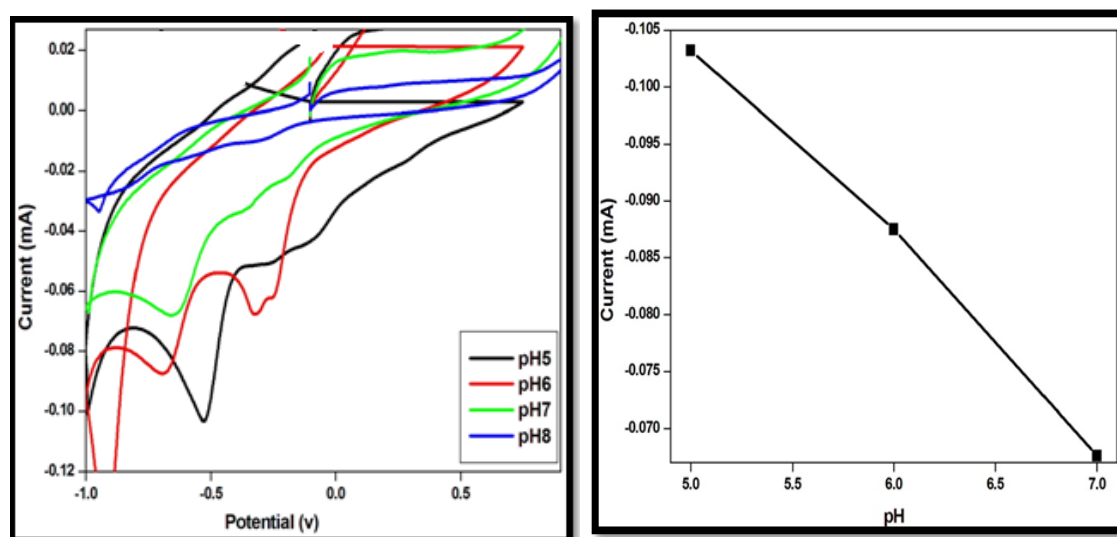
(a)
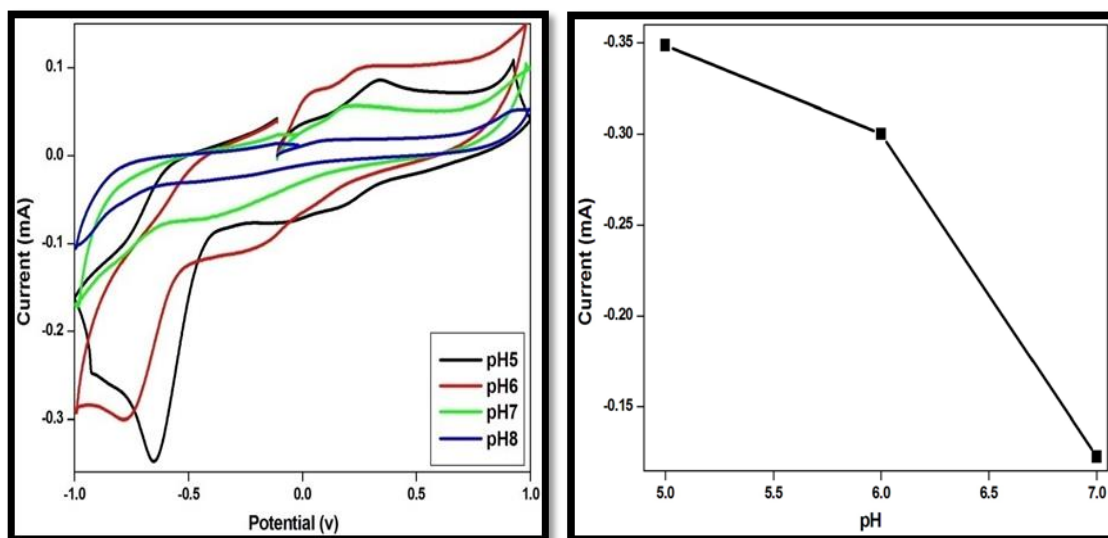
(b)

(c)

Figure.7.9. Effects of pH on the reduction peak current of (a) 230 μM o-NP and its linearity (b) 300 μM p-NP and its linearity (c) 260 μM m-NP and its linearity in 0.1M of PBS solution at the scan rate of 10 mV/s

The effect of electrolyte (PBS) pH on the electrochemical detection peak potential and current response of 230 μM of ortho-nitrophenol, 300 μM of para-nitrophenol and 260 μM of meta-nitrophenol at the 0.004 M of rGONS/β-CD/CuO modified glassy carbon electrode (GCE) is investigated with the 0.1 M of phosphate buffer solution (PBS) in the pH range from 5 to 8 and as shown in the Figure.7.9.(a-c)

202

respectively. The reduction peak potential corresponding to the ortho-, para- and meta-nitrophenol isomers are found to be shifted negatively with the increase in the electrolyte pH from 5 to 8, which shows that the electrocatalytic reduction process is assisted with proton transport [34] [36]. The calibration graph of pH dependent on the reduction peak current of ortho-, para- and meta-nitrophenol isomers reveals that the electrocatalytic reduction peak current corresponding to the detection of o- and p-NP isomers decreases with the increase in the electrolyte pH from 6 to 8, but in the case of meta-nitrophenol, the detection peak current increased with the increase in the pH from 5 to 6 and after that the peak current gets decreased. The highest reduction peak current of ortho-, para- and meta- nitrophenol isomers are observed for the PBS electrolyte with the pH value of 5.0, 5.0 and 6.0, respectively. Hence, the phosphate buffer solution with the pH of 5.0, 5.0 and 6.0 is selected as the optimized supporting electrolyte medium for the further electrochemical investigation of o-, p- and m-nitrophenol isomers respectively [34].
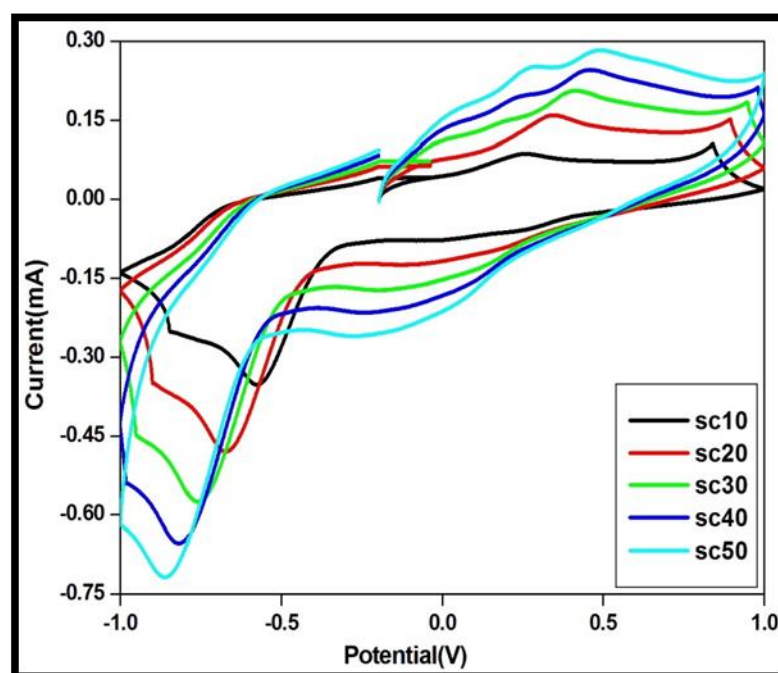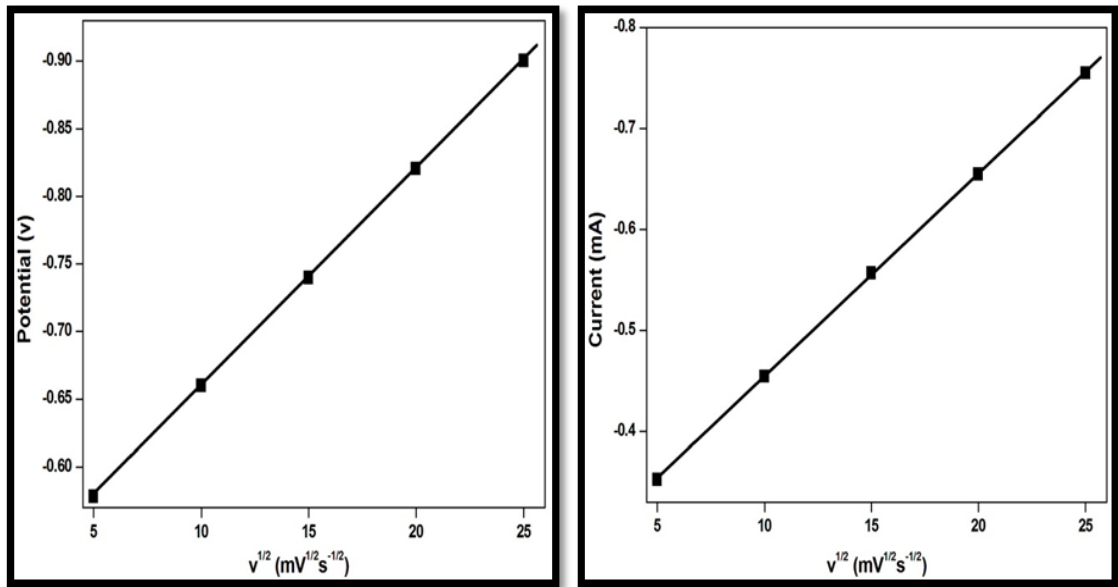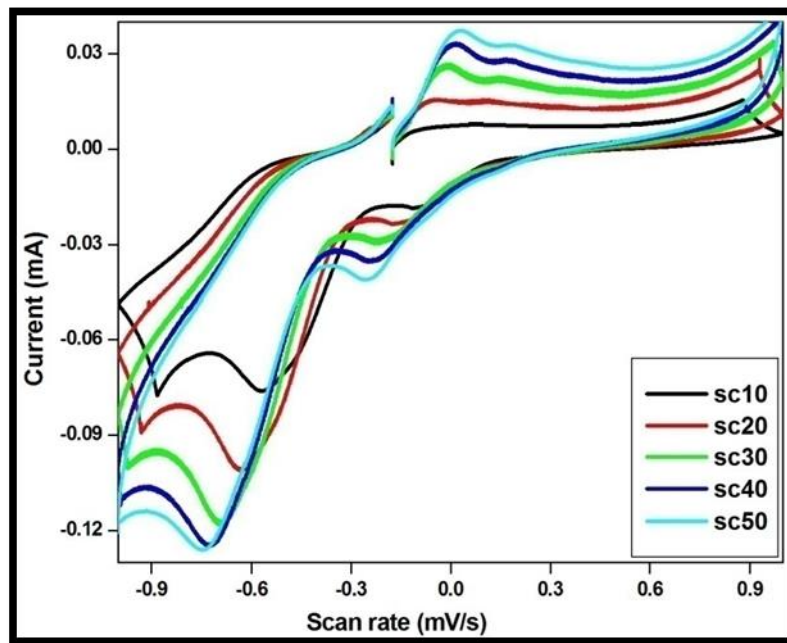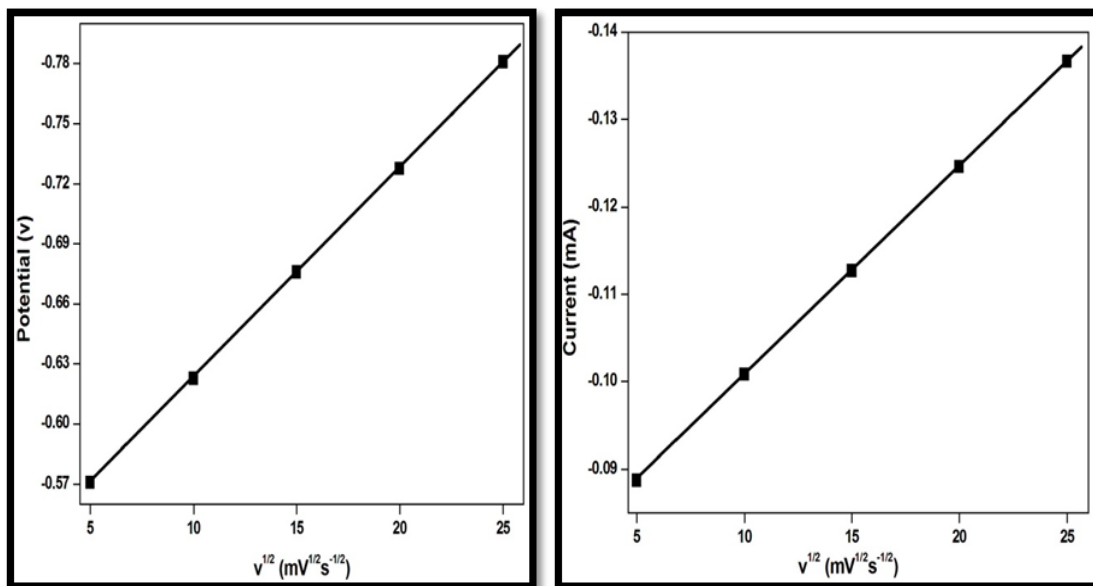
7.5.3. Effect of scan rate


(a)

(b)

(c)

(d)

(e)
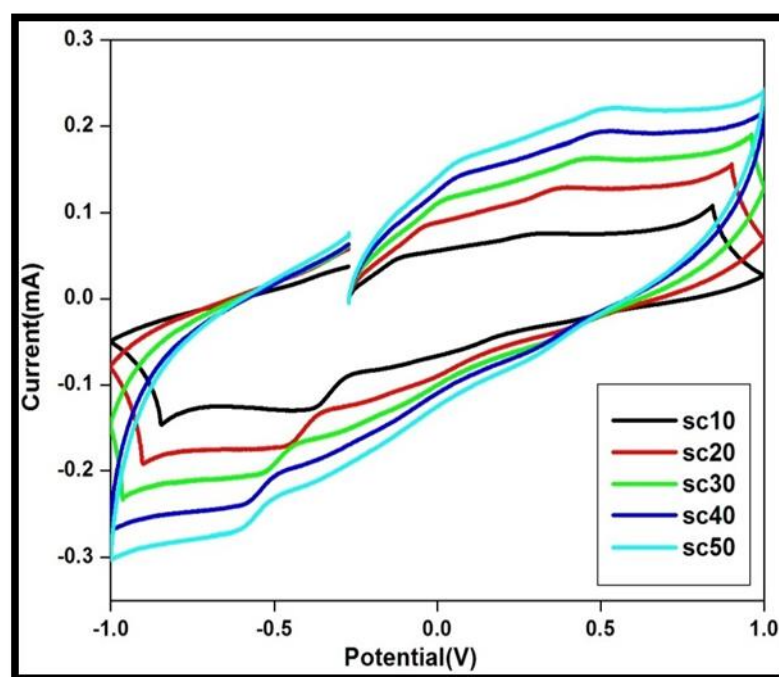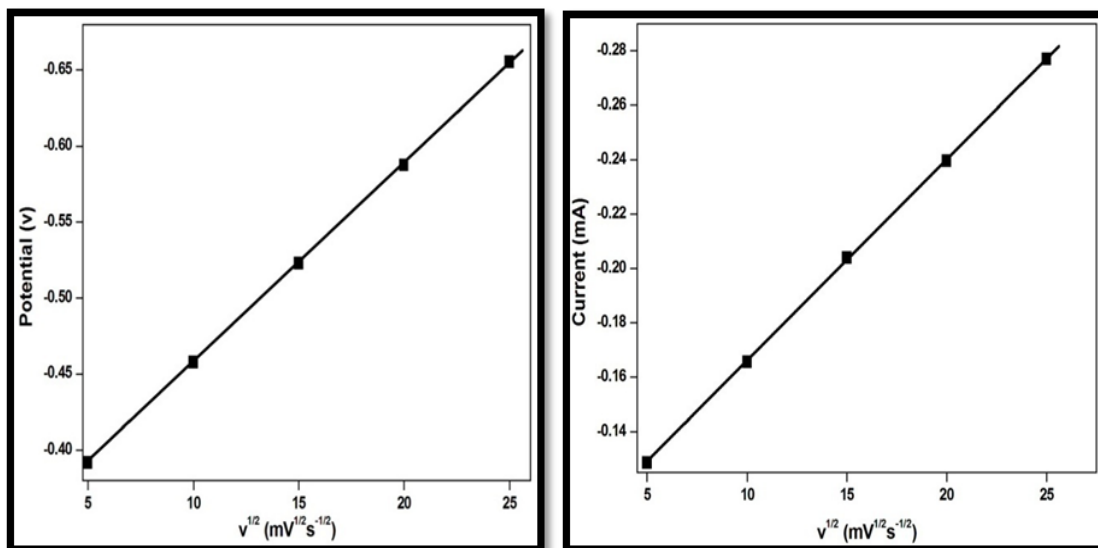
Figure.7.10. (a), (c), (e) Effect of scan rate on the redox current response for 230 µM, 300 µM and 260 µM of o-, p- and m-NP in 0.1 M PBS solution (b), (d), (f) Linear relationship between E_{pa}, I_{pa} and square root of scan rate

Figure.7.10.(a), (c) and (e) shows the influence of scan rate (v) on the electrochemical catalytic behaviour of 230 µM ortho-, 300 µM para- and 260 µM meta-nitrophenol at rGONS/β-CD/CuO nanocomposite modified GCE in 0.1 M of phosphate buffer solution (pH-5.0, 5.0 and 6.0) at the scan rate of 10 mV/s respectively. It is evident from the Figure.7.10.(a), (c) and (e) that the electrochemical redox peak current of o-, p- and m-NP isomers are gradually increases with the increase in the scan rate of the electrochemical process from 10 to 50 mV/s [34] [36]. The linearity graphs between the square root of scan rate to the corresponding redox peak potential and current of ortho-, para- and meta-nitrophenol isomers are plotted and are shown in the Figure.7.10.(b), (d) and (f) respectively. The redox peak current and potential of o-, p- and m-nitrophenol isomers are found to be linearly increased with the square root of scan rate in the range of 5-25 mV/s, which indicates that the electrochemical reduction and oxidation of ortho-, para- and meta-nitrophenol isomers at rGONS/β-CD/CuO modified GCE in a 0.1 M of phosphate buffer solution is a diffusion-controlled reversible electrode process [32] [36]. This phenomenon shows that the ortho-, para- and meta-nitrophenol sites accumulated on the surface of rGONS/β-CD/CuO

nanocomposites could be able to diffuse into the GCE electrode surface to undergo efficient electrochemical reactions [40].
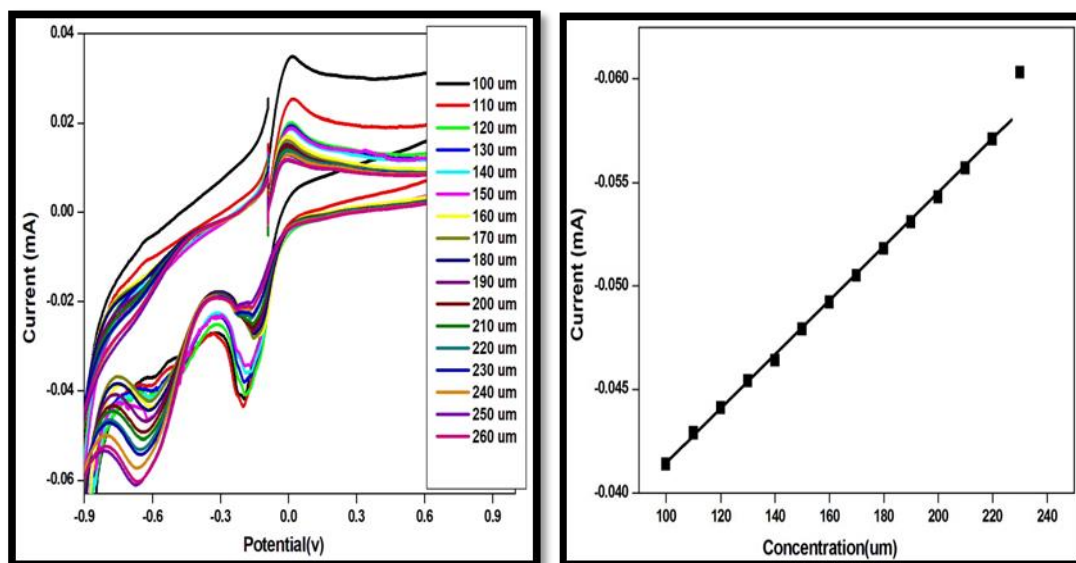
7.5.4. Effect of analyte (o-, p- and m-NP) concentration
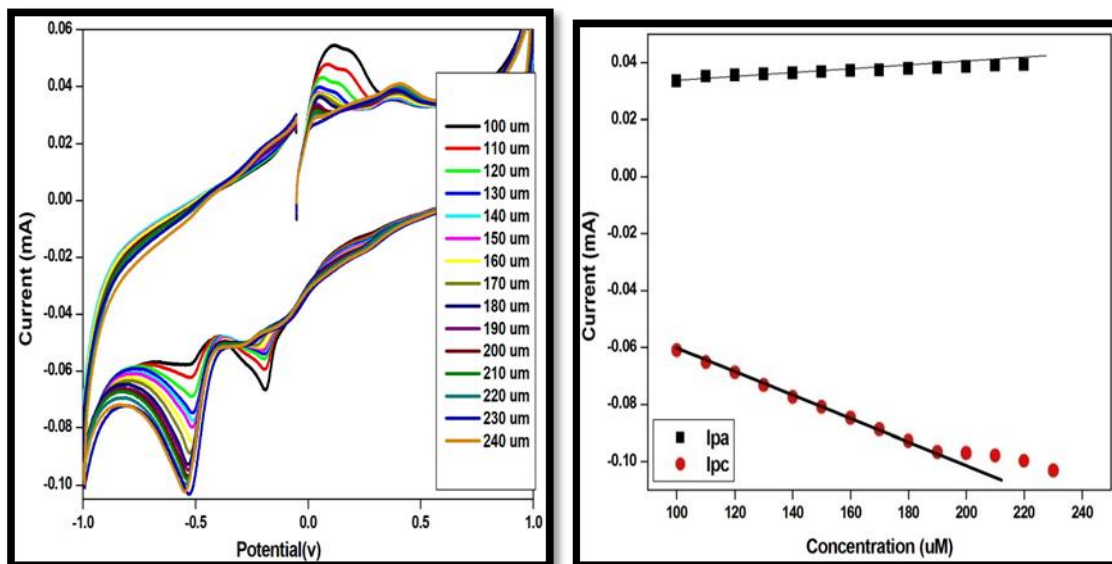
(a)
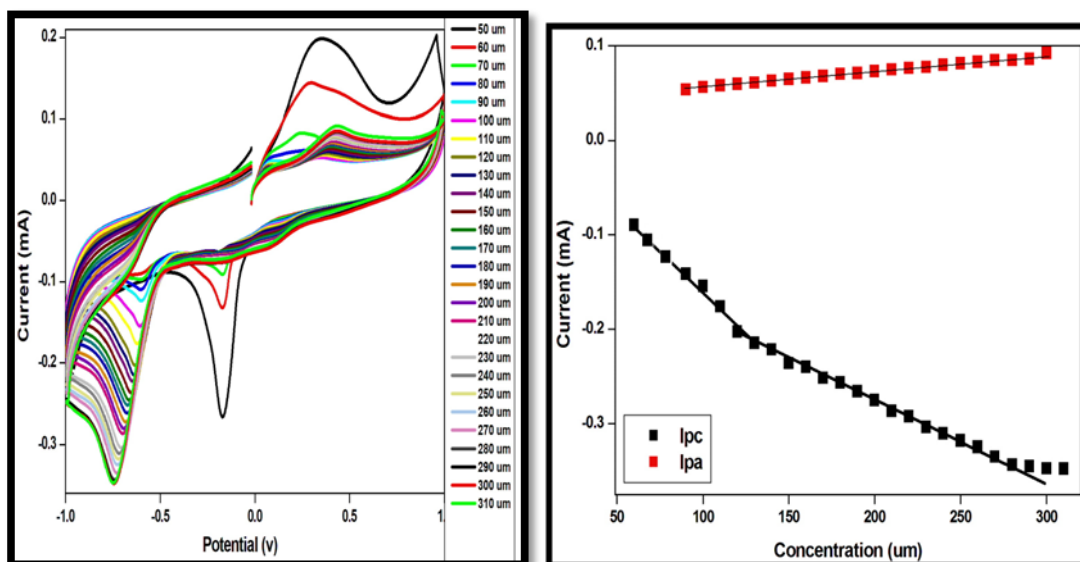
(b)

(c)

Figure.7.11. Cyclic voltagramm of rGONS/β-CD/CuO/GCE in 0.1 M PBS solution containing various concentration of (a) o-NP, (b) p-NP and (c) m-NP

The cyclic voltammetry study is carried out to investigate the sensitivity and detection limit of synthesized 0.004 M concentration of rGONS/β-CD/CuO nanocomposites modified GCE towards the detection of ortho-, para- and meta-nitrophenol isomers. The electrochemical detection of o-, p- and m-nitrophenol is performed in a series of solution containing different concentration of 100 μM to 240 μM ortho-, 60 μM to 310 μM para- and 100 μM to 260 μM meta-NP in a 0.1 M of phosphate buffer solution with the pH value of 5.0, 5.0 and 6.0 at the scan rate of 10 mV/s respectively and the obtained results are shown in the Figure.7.11.(a-c). The electrocatalytic redox peak current response of ortho-, para- and meta-nitrophenol isomers increases with the increase in the concentration from 100 μM to 230 μM ortho-, 60 μM to 300 μM para- and 100 μM to 250 μM meta-nitrophenol, respectively. With the further increase in the concentration of ortho-, para- and meta-nitrophenol above 230 μM, 300 μM and 250 μM, the redox peak current gradually decreases, which demonstrate that the accumulation of o-, p- and m-nitrophenol sites on the electrode surface reaches its saturation state that could decreases the electrocatalytic activity between the synthesized rGONS/β-CD/CuO modified GCE with the o-, p- and m-nitrophenol isomers. The calibration graph for the various concentration of o-, p- and m-NP and their corresponding detection current response is shown in the Figure.7.11.(a-

c). It is studied from the calibration graph that the rGONs/β-CD/CuO modified GCE displays a linear detection range from 100 to 190 μM for ortho-, and 100 μM to 210 μM for meta-nitrophenols. It also shows two linear range of detection from 60 μM to 90 μM and 120 μM to 280 μM for para-nitrophenol [38]. The sensitivity of the rGONS/β-CD/CuO modified GCE towards the detection of o-, p- and m-NP isomers are also obtained and the calculated values are 2.3 mAμM^{-1}cm^{-2}, 10.4 mAμM^{-1}cm^{-2} and 3.0 mAμM^{-1}cm^{-2} respectively. It is revealed from the electrochemical studies that the synthesized copper oxide nanoparticles decorated β-cyclodextrin functionalized graphene oxide nanocomposites shows the good electrochemical linear detection range and sensitivity against the para-nitrophenol isomer than the ortho- and meta-nitrophenol isomers.

7.6. CONCLUSION

The various concentrations (0.002 M, 0.004 M, 0.006 M, 0.008 M and 0.01 M) of uniformly dispersed copper oxide nanoparticles intercalated β-cyclodextrin functionalized reduced graphene oxide nanosheets (rGONS/β-CD/CuO) are successfully synthesized by wet chemical method and applied for the sensitive and quantitative determination of nitrophenol isomers through electrochemical technique. The decrease and increase in the FT-IR vibrational band intensities of rGONS, β-CD and CuO nanoparticles confirms the inclusion of β-CD and CuO nanoparticles on the surface of rGO nanosheets and further this inclusion enhances the electrocatalytic property. The XRD analysis revealed the decrease in the intensity and the broadening of the diffraction peaks of rGONS/β-CD with the increases in the concentration of copper II acetate monohydrate from 0.002 M to 0.01 M confirms the inclusion of high crystalline copper oxide nanoparticles on the surface of rGONS/β-CD. The morphological investigations such as SEM and HRTEM analysis confirmed that the nanocomposites synthesized using 0.004 M concentration of copper II acetate monohydrate are uniformly decorated with large number copper oxide nanoparticles without agglomeration. It also further confirms the inclusion of copper oxide nanoparticles and β-cyclodextrin polymer to rGO prevents the agglomeration of individual sheets of rGO. The cyclic voltammetric investigation on the detection of three different nitrophenol isomers using different concentrations of rGONS/β-CD/CuO nanocomposites modified GCE is studied and the results revealed that the nanocomposite with 0.004 M

concentration of copper oxide nanoparticles showed a better electrochemical behaviour with two linear range of detection for para-nitrophenol from 60 μm to 90 μm and 120 μm to 280 μm with a high sensitivity of 10.4 mAμM^{-1}cm^{-2}.

References

1. X. Huang, X. Qi, Graphene-based composites, Chem. Soc. Rev, 41, 666-686, (2012).

2. E.P. Randviir, D.A.C. Brownson, C.E. Banks, A decade of graphene research: production, applications and outlook, Mater. Today, 17, 426-432, (2014).

3. B. Unnikrishnan, S. Palanisamy, S.M. Chen, A simple electrochemical approach to fabricate a glucose biosensor based on graphene-glucose oxidase biocomposite, Biosens. Bioelectron, 39, 70-75, (2013).

4. P. Mahala, A. Kumar, S. Nayak, S. Behura, C. Dhanavantri, O. Jani, Graphene, conducting polymer and their composites as transparent and current spreading electrode in GaN solar cells, Superlattices Microstruct, 92, 366-373, (2016).

5. H. Gomez, M.K. Ram, F. Alvi, P. Villalb, E. Stefanakos, A. Kumar, Graphene conducting polymer nanocomposite as novel electrode for supercapacitors, J. Power Sources, 196, 4102-4108, (2011).

6. Q. Zhuo, Y. Ma, J. Gao, P. Zhang, Y. Xia, Y. Tian, X. Sun, J. Zhong, X. Sun, Facile synthesis of graphene/metal nanoparticle composites via self-catalysis reduction at room temperature, Inorg. Chem, 52, 3141-3147, (2013).

7. S. Zhang, Y. Shao, H. Liao, J. Liu, I.A. Aksay, G. Yin, Y. Lin, Graphene decorated with Pt/Au alloy nanoparticles: facile synthesis and promising application for formic acid oxidation, Chem. Mater, 23, 1079-1081, (2011).

8. X. Wu, Y. Xing, D. Pierce, J.X. Zhao, One-pot synthesis of reduced graphene oxide/metal (oxide) composites, ACS Appl. Mater. Interfaces, 9, 37962-7971, (2017).

9. S.H. Choi, J.K. Lee, Y.C. Kang, Three-dimensional porous graphene-metal oxide composite microspheres: preparation and application in Li-ion batteries, Nano Res, 8, 1584-1594, (2015).

10. Y. Guo, S. Guo, J. Ren, Y. Zhai, S. Dong, E. Wang, Cyclodextrin functionalized graphene nanosheets with high supramolecular recognition capability: synthesis

and host-guest inclusion for enhanced electrochemical performance, ACS Nano, 4, 4001-4010, (2010).

11. Vellaichamy Balakumar, Periakaruppan Prakash, synthesis of highly active and reusable ternary Ag-PPy-GO nanocomposite for catalytic oxidation of hydroquinone in aqueous solution, J. Catal, 344, 795-805, (2016).

12. Vellaichamy Balakumar, Periakaruppan Prakash, Silver nanoparticles embedded RGO-nanosponge for superior catalytic activity towards 4-nitrophenol reduction, RSC Adv, 6, 88837-88845, (2016).

13. Vellaichamy Balakumar, Periakaruppan Prakash, A facile, one-pot and ecofriendly synthesis of gold/silver nanobimetallics smartened rGO for enhanced catalytic reduction of hexavalent chromium, RSC Adv, 6, 57380-57388, (2016).

14. B. Vellaichamy, P. Periakaruppan, S.K. Ponnaiah, A new in-situ synthesized ternary CuNPs-PANI-GO nano composite for selective detection of carcinogenic hydrazine, Sensors Actuat, B, 245, 156-165, (2017).

15. B. Vellaichamy, S.K. Ponnaiah, P. Periakaruppan, An in-situ synthesis of novel Au@NG-PPy nanocomposite for enhanced electrocatalytic activity toward selective and sensitive sensing of catechol in natural samples, Sensors Actuat.B, 253, 392-399, (2017).

16. S. Palanisamy, K. Thangavelu, S.M. Chen, V. Velusamy, M.H. Chang, T.W. Chen, F.M.A. Hemaid, M.A. Ali, S.K. Ramaraj, Synthesis and characterization of polypyrrole decorated graphene/b-cyclodextrin composite for low level electrochemical detection of mercury (II) in water, Sens. Actuat, B, 243, 888-894, (2017).

17. G. Liu, B. Zheng, Y. Jiang, Y. Cai, J. Du, H. Yuan, D. Xiao, Improvement of sensitive CuO NFs–ITO nonenzymatic glucose sensor based on in situ electrospun fiber, Talanta, 101, 24-31, (2012).

18. X. Xiao, M. Wang, H. Li, Y. Pan, P. Si, Non-enzymatic glucose sensors based on controllable nanoporous gold/copper oxide nanohybrids,Talanta, 125, 366-371, (2014).

19. Y.Y. Yu, R.X. Xu, C. Gao, T. Luo, Y. Jia, J.H. Liu, X.J. Huang, novel 3D hierarchical cotton-candy-like CuO: surfactant-free solvothermal synthesis and application in As(III) removal, ACS Appl. Mater. Interfaces, 4, 1954-1962, (2012).

20. K.J. Choi, H.W. Jang, One-dimensional oxide nanostructures as gas-sensing materials: Review and issues, Sensors, 10, 4083-4099, (2010).

21. J. Liu, J. Jin, Z. Deng, S.Z. Huang, Z.Y. Hu, L. Wang, C. Wang, L.H. Chen, Y. Li, G.V.Tendeloo, B.L.J. Su, Tailoring CuO nanostructures for enhanced photocatalytic property, J. Colloid Interface Sci, 384, 1-9, (2012).

22. Huanshun Yin, Yunlei Zhou, Shiyun Ai, Xianggang Liu, Lusheng Zhu, Linan Lu, Electrochemical oxidative determination of 4-nitrophenol based on a glassy carbon electrode modified with a hydroxyapatite nanopowder, Microchim Acta, 169, 87-92, (2010).

23. M. Chen, Y. Meng, W. Zhang, J. Zhou, J. Xie, G. Diao, β-Cyclodextrin polymer functionalized reduced-graphene oxide: Application for electrochemical determination imidacloprid, Electrochimical Acta, 108, 1-9, (2013).

24. V. Ramalakshmi, J. Balavijayalakshmi, Investigation on embellishment of metal nanoparticles on graphene nanosheets and its sensing applications, Materials Science & Engineering, 14, 1-14, (2018).

25. Rajkumar Devasenathipathy, Shin Hung Tsai, Shen Ming Chen, Chelladurai Karuppiah, Raj Karthik, Sea Fue Wang, Electrochemical synthesis of β-Cyclodextrin functionalized silver nanoparticles and reduced graphene oxide composite for the determination of hydrazine, Electroanalysis, 28, 1-8, (2016).

26. Dipanwita Majumdar, Sonochemically synthesized beta-cyclodextrin functionalized graphene oxide and its efficient role in adsorption of water soluble brilliant green dye, J. Environ Anal Toxicol, 6, (2016).

27. Shanshan Wang, Yang Li, Xiaobin Fan, Fengbao Zhang, Guoliang Zhang, β-Cyclodextrin functionalized graphene oxide: an efficient and recyclable adsorbent for the removal of dye pollutants, Front. Chem. Sci. Eng, 9, 77-83, (2014).

28. Huawen Hu, H. John Xin, Hong Hu, Xiaowen Wang, Xinkun Lu, Organic liquids-responsive β-cyclodextrin-functionalized graphene-based fluorescence probe: label-free selective detection of tetrahydrofuran, Molecules, 19, 7459-7479, (2014).

29. Qiwen Chen, Luyan Zhang, Gang Chen, Facile preparation of graphene-copper nanoparticle composite by in situ chemical reduction for electrochemical sensing of carbohydrates, Anal. Chem, 84, 171-178, (2012).

30. Jaewon Hwang, Taeshik Yoon, Sung Hwan Jin, Jinsup Lee, Taek-Soo Kim, Soon Hyung Hong, Seokwoo Jeon, Enhanced mechanical properties of graphene/copper nanocomposites using a molecular-level mixing process,Adv. Mater, 25, 6724-6729, (2013).

31. Qi Zhang, Zhong Wu, Chen Xu, Lei Liu, Wenbin Hu, Temperature-driven growth of reduced graphene oxide/copper nanocomposites for glucose sensing, Nanotechnology, 27, 495603, (2016).

32. S.R. Kiran Kumar, G.P. Mamatha, H.B. Muralidhara, M.S. Anantha, S. Yallappa, B.S. Hungund, K. Yogesh Kumar, Highly efficient multipurpose graphene oxide embedded with copper oxide nanohybrid for electrochemical sensors and biomedical applications,J. Science: Advanced Materials and Devices, 2, (2017) 493-500.

33. Mehta, B.K., Meenal Chhajlani., Shrivastava, B.D., 2017. Green synthesis of silver nanoparticles and their characterization by XRD, J.Phy: Conf. Ser. 836 012050.

34. V. Vijayalakshmi, P. Selvakumar, K. Thangavelu, Shih-Wen Chen, C.K. Thomas Yang, E.B. Craig, Sumit Kumar Pramanik, Novel electrochemical synthesis of copper oxide nanoparticles decorated graphene-β-cyclodextrin

composite for trace-level detection of antibiotic drug metronidazole, Journal of colloid and interface science. 530 (2018) 37-45.

35. Xueshan Li, Yibo Zhao, Wei Wu, Jianfeng Chen, Guangwen Chu, Haikui Zou, Synthesis and characterizations of graphene-copper nanocomposites and their antifriction application, J. Industrial and Engineering Chemistry. 20 (2013) 2043-2049.

36. V. Balakumar, P. Prakash, P. Sathish Kumar, A new in-situ synthesized ternary CuNPs-PANI-GO nanocomposite for selective detection of caricogenic hydrazine, Sensors and Actuators B Chemical. 245 (2017) 156-165.

37. Y. Xing, Synthesis and electrochemical characterization of uniformly-dispersed high loading Pt nanoparticles on sonochemically-treated carbon nanotubes, J. Phys. Chem. B. 108 (2004) 19255-19259.

38. Yuchen Hui, Xiaoyan Ma, Xiuzhang Hou, Fang Chen, Jie Yu, Silver nanoparticles-β-cyclodextrin-graphene nanocomposites based biosensor for guanine and adenine sensing, Ionics. 21 (2014) 17517-1759.

39. Weilu Liu, Cong Li, Yue Gu, Liu Tang, Zhiquan Zhang, Ming Yang, One-step synthesis of β-cyclodextrin functionalized graphene/Ag nanocomposite and its application in sensitive determination of 4-nitrophenol, Electroanalysis. 25 (2013) 1-10.

40. Huanshun Yin, Yunlei Zhou, Shiyun Ai, Xianggang Liu, Lusheng Zhu, Linan Lu, Electrochemical oxidative determination of 4-nitrophenol based on a glassy carbon electrode modified with a hydroxyapatite nanopowder, Microchim Acta. 169 (2010) 87-92.